ChemComm

COMMUNICATION

View Article Online
View Journal | View Issue

Cite this: *Chem. Commun.*, 2014, 50, 12738

Received 4th August 2014,
Accepted 26th August 2014

DOI: 10.1039/c4cc06071g

www.rsc.org/chemcomm

Composition-tunable $Cu_2(Ge_{1-x},Sn_x)(S_{3-y},Se_y)$ colloidal nanocrystals: synthesis and characterization†

Yihui Wu,‡[a] Bin Zhou,‡[a] Mingrun Li,[a] Chi Yang,[ab] Wen-Hua Zhang*[a] and Can Li*[a]

A facile colloidal approach was developed to prepare cubic $Cu_2(Ge_{1-x},Sn_x)(S_{3-y},Se_y)$ nanocrystals (NCs) ($0 \le x \le 1$, $0 \le y \le 3$). The band gaps of the NCs can be tuned in the range of 1.35–2.45 eV by varying the chemical compositions, and the NCs display promising applications in solar energy utilization.

Colloidal semiconductor nanocrystals (NCs) have been widely studied and their great promising applications have been demonstrated in photovoltaics,[1] photodetectors,[2] light-emitting diodes (LEDs),[3] bioimaging,[4] thermoelectrics,[5] and so on. The field of semiconductor NCs synthesis has been dominated by binary systems, in which precise control over their morphology and crystal phase has been well developed.[6] In contrast, multi-component NCs offer the advantages of tunable optical and electronic properties that cannot be achieved in binary systems. Moreover, the band gaps of the multi-component NCs can be consecutively tailored by varying the ratios of the constituents over a wide range, providing an alternative to the quantum confinement effect that occurs for materials with sufficiently small size.[7] Currently, it is highly desirable to extend the colloidal synthesis to the multi-component NCs,[8] while the success is very limited compared to the binary system.

As environmentally benign materials with the capability of band gap tailoring in a wide range, Cu-based ternary and quaternary chalcogenides have received considerable interest in electronics. High-quality Cu-based multi-component NCs, including $Cu_2(S,Se)$,[8a] $CuIn(Te,Se)_2$,[8b] $Cu_2Ge(S,Se)_3$,[8c] $Cu_2Zn(Cd)Sn(S,Se)_4$,[9] $Cu_2Zn(Sn,Ge)S_4$,[10] and $Cu(In,Ga)Se_2$,[11] have recently been prepared *via* colloidal chemistry, showing a remarkable promise in photovoltaic cells.[9b,c,10,11] Nevertheless, in comparison with the binary ones, it remains a much bigger challenge to balance the reactivity of each precursor for a multi-component system.

Cu_2MX_3 (M = Ge, Sn, X = S, Se) bulk materials are p-type semiconductors with a band gap of 1.5 eV,[12] 0.78 eV,[13] 0.8–1.35 eV[14] and 0.8–1.1 eV[15] for Cu_2GeS_3, Cu_2GeSe_3, Cu_2SnS_3 and Cu_2SnSe_3, respectively. All of these materials exhibit a high absorption coefficient and high carrier mobility, which make them attractive for fabricating photoelectronic devices. Cabot *et al.*[16] have developed the colloidal synthesis of Cu_2GeSe_3 nanoparticles along with their thermoelectric properties. Meng *et al.*[17] have prepared $Cu_2Sn(S_x,Se_{1-x})_3$ NCs with tunable composition in the range of $0 < x \le 1$. We have realized the synthesis of a family of monodisperse $Cu_2Ge(S_{3-x},Se_x)$ alloyed colloidal NCs with well-controlled composition and engineered their band gaps across the entire range ($0 \le x \le 3$).[8c] However, due to the different reactivity of Ge and Sn precursors in colloidal synthesis, fabrication of monodispersed $Cu_2(Ge_{1-x},Sn_x)(S_{3-y},Se_y)$ NCs with tunable Ge–Sn compositions by colloidal chemistry remains undeveloped. In this work, we report the successful synthesis of $Cu_2(Ge_{1-x},Sn_x)(S_{3-y},Se_y)$ ($0 \le x \le 1$, $0 \le y \le 3$) NCs in a highly controlled way *via* colloidal chemistry. The chemical compositions of the resulting NCs are tunable in the entire compositional range ($0 \le x \le 1$, $0 \le y \le 3$), accompanied by the simultaneous tailoring of their band gaps in the range of 1.35–2.45 eV. The application potential of the as-synthesized NCs as photovoltaic materials was finally demonstrated by fabricating nanocrystal solar cells consisting of n-type CdS nanorods and p-type $Cu_2(Ge_{1-x},Sn_x)(S_{3-y},Se_y)$ ($0 \le x \le 1$, $0 \le y \le 3$) NCs through a cost-effective solution process.

The synthesis of $Cu_2(Ge_{1-x},Sn_x)(S_{3-y},Se_y)$ colloidal NCs was performed on the basis of our previous report incorporated with modifications.[8c] Typically, copper(II) acetylacetonate [$Cu(acac)_2$] and tin(II) bromide ($SnBr_2$) were dissolved in dried oleylamine (OLA). The flask was heated to 120 °C under vacuum, into which a specific ratio of germanium tetrachloride ($GeCl_4$)/tin bromide ($SnBr_2$) was then injected. Meanwhile, S and SeO_2 were dissolved respectively in dried OLA and octadecylene (ODE), and were then injected into the above OLA solution at 160 °C. The mixed solution was finally heated to 280 °C and the reaction lasted

[a] *State Key Laboratory of Catalysis, Dalian Institute of Chemical Physics, Chinese Academy of Sciences, Dalian National Laboratory for Clean Energy, Dalian 116023, China. E-mail: whzhang@dicp.ac.cn, canli@dicp.ac.cn*
[b] *Department of Materials Science and Engineering, University of Science and Technology of China, Hefei 230026, China*

† Electronic supplementary information (ESI) available: Experimental details, XRD patterns, TEM and HRTEM images, EDX spectra, UV-vis spectra and Tauc plots. See DOI: 10.1039/c4cc06071g

‡ These authors contributed equally to this work.

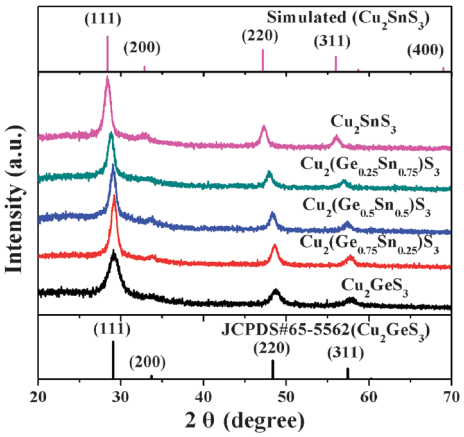

Fig. 1 XRD patterns of the $Cu_2(Ge_{1-x},Sn_x)S_3$ NCs with various Sn/(Ge + Sn) ratios ($0 \leq x \leq 1$).

for 2 hours to yield the targeted NCs. Full experimental details can be found in the ESI.†

Fig. 1 presents the powder X-ray diffraction (XRD) patterns of the as-synthesized $Cu_2(Ge_{1-x},Sn_x)S_3$ NCs with $0 \leq x \leq 1$. All diffraction peaks of the Cu_2GeS_3 NCs match well with the major peaks of cubic-structured Cu_2GeS_3 (JCPDS No. 65-5562, $F\bar{4}3m$). For Cu_2SnS_3 NCs, it was found that our XRD patterns cannot be indexed to any existing patterns in the standard JCPDS database. Therefore, a diffraction pattern was simulated for Cu_2SnS_3 on the basis of the $F\bar{4}3m$ cubic structure with an experimental lattice parameter of $a = b = c = 5.442$ Å. As presented in Fig. 1, the experimental XRD pattern matches very well with the simulated one (details are given in Table S1, ESI†), indicating that the as-synthesized Cu_2SnS_3 exhibits the same cubic structure ($F\bar{4}3m$) as Cu_2GeS_3, which is in line with the reported results.[18] Additionally, the major diffraction peaks systematically shift toward lower angles with increasing Sn contents, meaning that the larger Sn atoms have replaced the smaller Ge atoms in the lattices of the resulting NCs. Very importantly, no additional peak or peak splitting can be detected by XRD, which rules out the possibility of phase separation that often takes place in the preparation of multi-component colloidal NCs.[7] Elemental line scan of $Cu_2(Ge_{0.5},Sn_{0.5})S_3$ NCs (Fig. S1, ESI†) disclosed the homogenous distribution of the four elements involved. These results demonstrate that pure phase $Cu_2(Ge_{1-x},Sn_x)S_3$ ($0 \leq x \leq 1$) NCs with cubic structure were successfully obtained, featured by their highly tunable compositions across the entire range ($0 \leq x \leq 1$). This is in good agreement with the behavior of homogenous alloys,[19] thus confirming the formation of alloyed NCs with homogeneous distribution of Ge and Sn in the $Cu_2(Ge_{1-x},Sn_x)S_3$ matrix.

Transmission electron microscopy (TEM) was then performed to reveal the microstructures of the $Cu_2(Ge_{1-x},Sn_x)S_3$ ($0 \leq x \leq 1$) NCs, as shown in Fig. 2. The low-magnification TEM displays a uniform size distribution of the $Cu_2(Ge_{1-x},Sn_x)S_3$ ($0 \leq x \leq 1$) NCs. The polycrystalline selected area electron diffraction (SAED) patterns of the NCs show clearly three diffraction rings that match well with the (111), (220), and (311) lattice planes of the cubic $Cu_2(Ge_{1-x},Sn_x)S_3$, which is consistent with the XRD results (shown in Fig. 1). High-resolution transmission electron

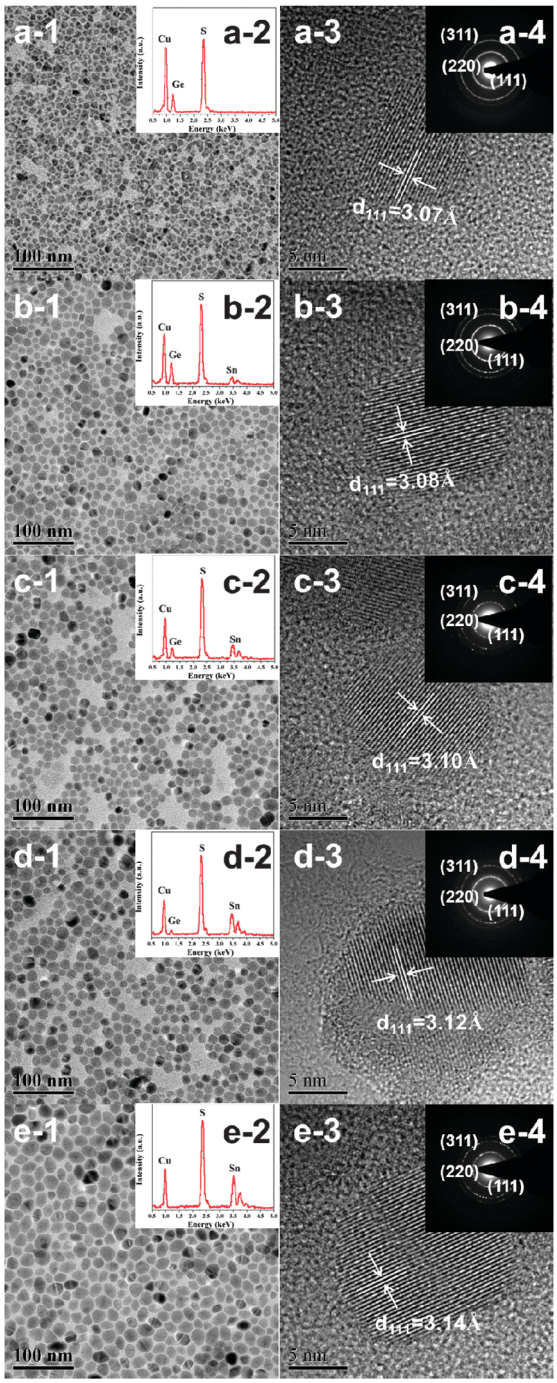

Fig. 2 TEM analysis of the $Cu_2(Ge_{1-x},Sn_x)S_3$ ($0 \leq x \leq 1$) NCs. (a)–(e) denote respectively the samples Cu_2GeS_3, $Cu_2(Ge_{0.75},-Sn_{0.25})S_3$, $Cu_2(Ge_{0.5},Sn_{0.5})S_3$, $Cu_2(Ge_{0.25},Sn_{0.75})S_3$, and Cu_2SnS_3 NCs. 1, 2, 3, and 4 represent the corresponding low magnification TEM images, EDS spectra, HRTEM images and SAED patterns of these samples.

microscopy (HRTEM) images show that all $Cu_2(Ge_{1-x},Sn_x)S_3$ NCs are highly crystalline with continuous lattice fringes across the NC. Moreover, the interplanar crystal spacing of d_{111} increases from 0.307 nm to 0.314 nm with increasing Sn contents, confirming that the larger Sn atoms have successfully substituted the smaller Ge atoms in the lattices of the resulting NCs. Elemental composition of the as-prepared $Cu_2(Ge_{1-x},Sn_x)S_3$ NCs was analyzed by energy

dispersive X-ray spectroscopy (EDS) (Table S2, ESI†), disclosing that all samples have a similar Cu/S molar ratio of ~2/3, and the increase of Sn content was accompanied by the decrease of Ge content in the range of $0 \leq x \leq 1$. Therefore, we have achieved the controlled growth of well-crystalline $Cu_2(Ge_{1-x},Sn_x)S_3$ NCs with a narrow size distribution (Fig. S2, ESI†) and varied Sn/Ge ratios across the whole compositional range ($0 \leq x \leq 1$). It is well known that semiconducting alloys are characteristic of the tunable band gaps that change in a nearly linear manner with their compositions.[19] UV-vis-NIR absorption spectra of $Cu_2(Ge_{1-x},Sn_x)S_3$ NCs ($0 \leq x \leq 1$) were therefore acquired to study their optical properties and to determine their band gaps. A clear solution of each $Cu_2(Ge_{1-x},Sn_x)S_3$ ($0 \leq x \leq 1$) NC sample showed a continuous absorption spectrum spanning the whole visible spectrum (shown in Fig. 3a). Tauc plots (Fig. S3, ESI†) were performed to assess the optical band gaps with a relationship of α^2 *versus* energy, revealing that Cu_2GeS_3 NCs exhibit a direct band gap of 2.45 eV. Moreover, as expected, the band gap energies are progressively reduced from 2.45 eV to 1.57 eV upon increasing the Sn content in $Cu_2(Ge_{1-x},Sn_x)S_3$ NCs ($0 \leq x \leq 1$), presenting a nearly linear relationship between the band gaps and the Sn/Ge contents (Fig. 3b). These results further manifest the successful formation of homogeneous alloyed $Cu_2(Ge_{1-x},Sn_x)S_3$ NCs ($0 \leq x \leq 1$) in the present experiment.

To further expand the present colloidal synthesis of $Cu_2(Ge_{1-x},Sn_x)S_3$ NCs to a complex multi-component system, we have exploited the synthesis of $Cu_2(Ge_{1-x},Sn_x)(S_{3-y},Se_y)$ NCs ($0 \leq x \leq 1$, $0 \leq y \leq 3$), where the Ge/Sn molar ratio was kept at 1 (*i.e.*, $x = 0.5$) for simplicity. Fig. 3c shows the XRD patterns of $Cu_2(Ge_{0.5},Sn_{0.5})(S_{3-y},Se_y)$ ($0 \leq y \leq 3$) NCs. No diffraction peaks due to impurities can be observed and the major reflection peaks systematically shifted toward lower angles with increasing Se content, again indicating that the larger Se atoms have successfully incorporated into the lattice of the resulting NCs. TEM, HRTEM, SAED, EDS (Fig. S4 and Table S2, ESI†), and UV-vis-NIR absorption spectra (Fig. S5, ESI†) all confirm the formation of the alloyed $Cu_2(Ge_{0.5},Sn_{0.5})(S_{3-y},Se_y)$ ($0 \leq y \leq 3$) NCs with a narrow size distribution (Fig. S6, ESI†). Moreover, the band gap energies further varied gradually from 1.95 eV to 1.35 eV with increasing Se content (Fig. 3d) with a nearly linear relationship. Therefore, we have presented a facile solution approach for complete synthesis of $Cu_2(Ge_{1-x},Sn_x)(S_{3-y},Se_y)$ ($0 \leq x \leq 1$, $0 \leq y \leq 3$) NCs in a highly controlled way, achieving control over their chemical compositions, optical properties, and band gaps across the entire compositional range ($0 \leq x \leq 1$, $0 \leq y \leq 3$).

We then turned to study the photoelectrochemical (PEC) properties of the $Cu_2(Ge_{1-x},Sn_x)(S_{3-y},Se_y)$ ($0 \leq x \leq 1$, $0 \leq y \leq 3$) NCs by measuring the transient photocurrents of the NC films on fluoride tin oxide (FTO) substrates in a photoelectrochemical cell. Photocurrent obtained from the $Cu_2(Ge_{0.5},Sn_{0.5})(S_2,Se)$ NCs electrode was negative (cathode current) (Fig. 4a), indicative of p-type semiconductor behaviour.[20] And the photocurrents of the NC film increased rapidly upon illumination, and dropped immediately to their pre-illumination values without apparent degradation over many cycles upon turning the illumination on and off. Similar phenomena were also observed for other $Cu_2(Ge_{1-x},Sn_x)(S_{3-y},Se_y)$ ($0 \leq x \leq 1$, $0 \leq y \leq 3$) NC films (Fig. S7, ESI†). Therefore, the $Cu_2(Ge_{1-x},Sn_x)(S_{3-y},Se_y)$ NCs are sensitive to light illumination and are chemically stable under experimental conditions.

Currently, the demand for low-cost photovoltaic cells boosts the development of solar cells consisting of semiconductor NCs *via* scalable, solution-processed device fabrication.[21] We have hence employed the p-type $Cu_2(Ge_{0.5},Sn_{0.5})(S_2,Se)$ NCs as a model material to assemble photovoltaic devices due to their relative simplicity in the formation of smooth nanocrystal films and their relatively suitable band gap (1.75 eV). The devices were fabricated with the configuration of FTO/TiO_2 compact layer (c-TiO_2)/CdS nanorods (NRs)[22]/$Cu_2(Ge_{0.5},Sn_{0.5})(S_2,Se)$ NCs/Spiro-MeOTAD[23]/Au. The $Cu_2(Ge_{0.5},Sn_{0.5})(S_2,Se)$ NCs were deposited by spin coating of a nanocrystal solution *via* a layer-by-layer approach. A typical cross-sectional SEM image (Fig. S8, ESI†) indicates that the resulting NC film has a thickness of ~1000 nm, slightly greater than the height of the CdS NRs (~800 nm), thus separating the top of the CdS NRs from

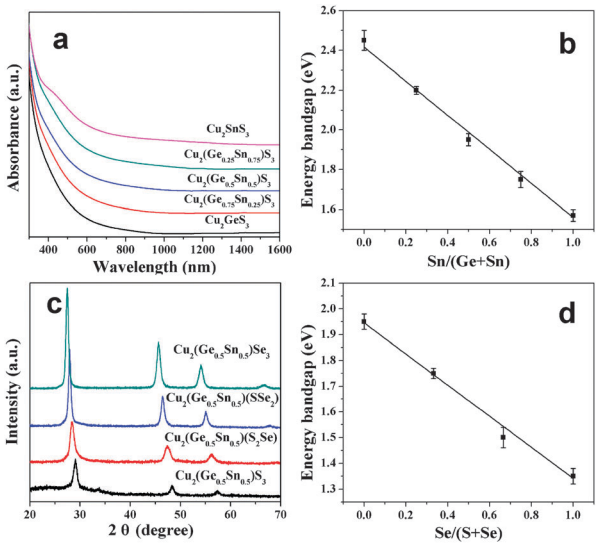

Fig. 3 (a) UV-vis-NIR absorption spectra of the $Cu_2(Ge_{1-x},Sn_x)S_3$ NCs with various Sn/Ge ratios ($0 \leq x \leq 1$), (b) relationship between the band gaps of the $Cu_2(Ge_{1-x},Sn_x)S_3$ NCs and the contents of Sn/Ge in the products, (c) XRD patterns of the $Cu_2(Ge_{0.5},Sn_{0.5})(S_{3-y},Se_y)$ NCs with various Se/(S + Se) ratios ($0 \leq y \leq 3$), and (d) relationship between the band gaps of the $Cu_2(Ge_{0.5},Sn_{0.5})(S_{3-y},Se_y)$ NCs and the contents of Se/S in the products.

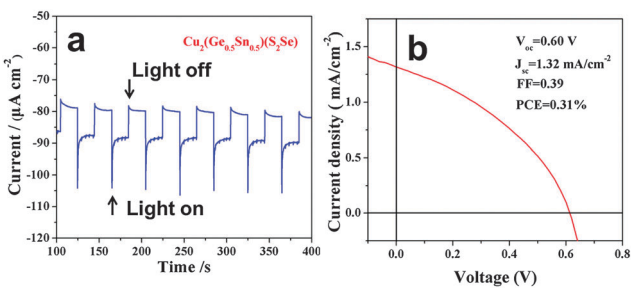

Fig. 4 (a) Transient photocurrent response of the $Cu_2(Ge_{0.5},Sn_{0.5})$ (S_2,Se) NC, and (b) *J*–*V* curves of the solar cells with the configuration of FTO/c-TiO_2/CdS NRs/$Cu_2(Ge_{0.5},Sn_{0.5})(S_2,Se)$ NCs/Spiro-MeOTAD/Au.

the Spiro-MeOTAD/Au to avoid the short circuit. The corresponding device performances are characterized by current density–voltage (J–V) measurements under simulated AM 1.5 G (100 mW cm^{-2}) solar irradiation in air. Fig. 4b presents the photovoltaic characteristics of $Cu_2(Ge_{0.5},Sn_{0.5})(S_2,Se)$ NC-based solar cells. An open-circuit voltage (V_{oc}) of 0.60 V, a short-circuit current density (J_{sc}) of 1.32 mA cm^{-2}, and a fill factor (FF) of 0.39 were obtained, resulting in a power conversion efficiency (η) of 0.31%. A control cell device was also fabricated under the same conditions as the NC cell while no NCs were involved, showing negligible efficiency. Therefore, these results demonstrate the application potential of the $Cu_2(Ge_{1-x},Sn_x)(S_{3-y},Se_y)$ NCs in solar energy conversions. The efficiency is low for the present device. One possible reason is that the solution processed NCs are capped by organic ligands, which results in insulating barriers between NCs that militate against efficient carrier transports when processed into films, thus decreasing the photocurrent generated from them. Moreover, small NCs show high specific surface areas, thus a large interface exists in the resulting NC film, leading to high charge recombination probability, thereby deteriorating the device performance. It is expected that the device performance could be improved significantly for the NC-based photovoltaic cells by optimizing the device fabrication, for example, by annealing the nanocrystal films using Se vapour[9c,e] to form large crystal grains.

In summary, we have shown a complete synthesis of $Cu_2(Ge_{1-x},Sn_x)(S_{3-y},Se_y)$ NCs in a highly controllable way across the entire compositional range ($0 \le x \le 1$, $0 \le y \le 3$) *via* a facile colloidal approach. The cubic-structured $Cu_2(Ge_{1-x},Sn_x)$–(S_{3-y},Se_y) NCs displayed uniform size distributions along with the highly crystalline nature. The band gaps of the NCs could be effectively tuned in the range of 1.35–2.45 eV by varying their chemical compositions. Preliminary application in photovoltaic devices has been demonstrated by using $Cu_2(Ge_{1-x},Sn_x)(S_{3-y},Se_y)$ NCs as a light absorber in fully solution-processed solar cells, generating 0.31% power conversion efficiency under AM1.5 illumination. These results manifest that $Cu_2(Ge_{1-x},Sn_x)(S_{3-y},Se_y)$ NCs are potential candidates for solar energy utilization.

We are grateful for financial support from the ''Hundred Talents Program'' of the Chinese Academy of Sciences and the National Science Foundation of China (No. 20873141)

Notes and references

1 (*a*) W. U. Huynh, *Science*, 2002, **295**, 2425; (*b*) A. G. Pattantyus-Abraham, I. J. Kramer, A. R. Barkhouse, X. Wang, G. Konstantatos, R. Debnath, L. Levina, I. Raabe, M. K. Nazeeruddin, M. Grätzel and E. H. Sargent, *ACS Nano*, 2010, **4**, 3374; (*c*) Z. Yang, C.-Y. Chen, P. Roy and H.-T. Chang, *Chem. Commun.*, 2011, **47**, 9561; (*d*) X. Lu, Z. Zhuang, Q. Peng and Y. Li, *Chem. Commun.*, 2011, **47**, 3141.

2 (*a*) V. Sukhovatkin, S. Hinds, L. Brzozowski and E. H. Sargent, *Science*, 2009, **324**, 1542; (*b*) S. A. McDonald, G. Konstantatos, S. Zhang, P. W. Cyr, E. J. D. Klem, L. Levina and E. H. Sargent, *Nat. Mater.*, 2005, **4**, 138.

3 (*a*) S. K. Panda, S. G. Hickey, H. V. Demir and A. Eychmüller, *Angew. Chem., Int. Ed.*, 2011, **50**, 4432; (*b*) N. Tessler, V. Medvedev, M. Kazes, S. Kan and U. Banin, *Science*, 2002, **295**, 1506.

4 W. Li, R. Zamani, P. Rivera Gil, B. Pelaz, M. Ibáñez, D. Cadavid, A. Shavel, R. A. Alvarez-Puebla, W. J. Parak, J. Arbiol and A. Cabot, *J. Am. Chem. Soc.*, 2013, **135**, 7098.

5 (*a*) T. C. Harman, P. J. Taylor, M. P. Walsh and B. E. LaForge, *Science*, 2002, **297**, 2229; (*b*) Y. Sun, H. Cheng, S. Gao, Q. Liu, Z. Sun, C. Xiao, C. Wu, S. Wei and Y. Xie, *J. Am. Chem. Soc.*, 2012, **134**, 20294.

6 (*a*) T.-T. Zhuang, F.-J. Fan, M. Gong and S.-H. Yu, *Chem. Commun.*, 2012, **48**, 9762; (*b*) Z. Li and X. Peng, *J. Am. Chem. Soc.*, 2011, **133**, 6578; (*c*) S. Liu, X. Guo, M. Li, W.-H. Zhang, X. Liu and C. Li, *Angew. Chem., Int. Ed.*, 2011, **50**, 12050; (*d*) M. A. Franzman, C. W. Schlenker, M. E. Thompson and R. L. Brutchey, *J. Am. Chem. Soc.*, 2010, **132**, 4060; (*e*) L. Liu, Z. Zhuang, T. Xie, Y.-G. Wang, J. Li, Q. Peng and Y. Li, *J. Am. Chem. Soc.*, 2009, **131**, 16423.

7 M. D. Regulacio and M.-Y. Han, *Acc. Chem. Res.*, 2010, **43**, 621.

8 (*a*) J.-J. Wang, D.-J. Xue, Y.-G. Guo, J.-S. Hu and L.-J. Wan, *J. Am. Chem. Soc.*, 2011, **133**, 18558; (*b*) S. Kim, M. Kang, S. Kim, J.-H. Heo, J. H. Noh, S. H. Im, S. I. Seok and S.-W. Kim, *ACS Nano*, 2013, **7**, 4756; (*c*) C. Yang, B. Zhou, S. Miao, C. Yang, B. Cai, W.-H. Zhang and X. Xu, *J. Am. Chem. Soc.*, 2013, **135**, 5958.

9 (*a*) A. Singh, S. Singh, S. Levcenko, T. Unold, F. Laffir and K. M. Ryan, *Angew. Chem., Int. Ed.*, 2013, **52**, 9120; (*b*) J. Zhong, Z. Xia, C. Zhang, B. Li, X. Liu, Y.-B. Cheng and J. Tang, *Chem. Mater.*, 2014, **26**, 3573; (*c*) Q. Guo, G. M. Ford, W.-C. Yang, B. C. Walker, E. A. Stach, H. W. Hillhouse and R. Agrawal, *J. Am. Chem. Soc.*, 2010, **132**, 17384; (*d*) U. Ghorpade, M. Suryawanshi, S. W. Shin, K. Gurav, P. Patil, S. Pawar, C. W. Hong, J. H. Kim and S. Kolekar, *Chem. Commun.*, 2014, **50**, 11258; (*e*) Y. Cao, M. S. Denny, J. V. Caspar, W. E. Farneth, Q. Guo, A. S. Ionkin, L. K. Johnson, M. Lu, I. Malajovich, D. Radu, H. D. Rosenfeld, K. R. Choudhury and W. Wu, *J. Am. Chem. Soc.*, 2012, **134**, 15644; (*f*) F.-J. Fan, Y.-X. Wang, X.-J. Liu, L. Wu and S.-H. Yu, *Adv. Mater.*, 2012, **24**, 6158; (*g*) F.-J. Fan, L. Wu and S.-H. Yu, *Energy Environ. Sci.*, 2014, **7**, 190; (*h*) F.-J. Fan, B. Yu, Y.-X. Wang, Y.-L. Zhu, X.-J. Liu, S.-H. Yu and Z. Ren, *J. Am. Chem. Soc.*, 2011, **133**, 15910.

10 G. M. Ford, Q. Guo, R. Agrawal and H. W. Hillhouse, *Chem. Mater.*, 2011, **23**, 2626.

11 M. G. Panthani, V. Akhavan, B. Goodfellow, J. P. Schmidtke, L. Dunn, A. Dodabalapur, P. F. Barbara and B. A. Korgel, *J. Am. Chem. Soc.*, 2008, **130**, 16770.

12 I. Tsuji, Y. Shimodaira, H. Kato, H. Kobayashi and A. Kudo, *Chem. Mater.*, 2010, **22**, 1402.

13 G. Marcano, D. B. Bracho, C. Rincón, G. S. n. Pérez and L. Nieves, *J. Appl. Phys.*, 2000, **88**, 822.

14 Y.-T. Zhai, S. Chen, J.-H. Yang, H.-J. Xiang, X.-G. Gong, A. Walsh, J. Kang and S.-H. Wei, *Phys. Rev. B: Condens. Matter Mater. Phys.*, 2011, **84**, 075213.

15 (*a*) M. E. Norako, M. J. Greaney and R. L. Brutchey, *J. Am. Chem. Soc.*, 2012, **134**, 23; (*b*) J.-j. Wang, P. Liu, C. C. Seaton and K. M. Ryan, *J. Am. Chem. Soc.*, 2014, **136**, 7954.

16 M. Ibáñez, R. Zamani, W. Li, D. Cadavid, S. Gorsse, N. A. Katcho, A. Shavel, A. M. López, J. R. Morante, J. Arbiol and A. Cabot, *Chem. Mater.*, 2012, **24**, 4615.

17 Q. Liang, L. Han, X. Deng, C. Yao, J. Meng, X. Liu and J. Meng, *CrystEngComm*, 2014, **16**, 4001.

18 Q. Liu, Z. Zhao, Y. Lin, P. Guo, S. Li, D. Pan and X. Ji, *Chem. Commun.*, 2011, **47**, 964.

19 L. Vegard and H. Schjelderup, *Phys. Z.*, 1917, **18**, 93.

20 D. H. Webber and R. L. Brutchey, *J. Am. Chem. Soc.*, 2012, **134**, 1085.

21 (*a*) E. H. Sargent, *Nat. Photonics*, 2009, **3**, 325; (*b*) I. J. Kramer and E. H. Sargent, *Chem. Rev.*, 2014, **114**, 863; (*c*) J. Y. Kim, O. Voznyy, D. Zhitomirsky and E. H. Sargent, *Adv. Mater.*, 2013, **25**, 4986; (*d*) J. Tang, K. W. Kemp, S. Hoogland, K. S. Jeong, H. Liu, L. Levina, M. Furukawa, X. Wang, R. Debnath, D. Cha, K. W. Chou, A. Fischer, A. Amassian, J. B. Asbury and E. H. Sargent, *Nat. Mater.*, 2011, **10**, 765.

22 C. Yang, S. Liu, M. Li, X. Wang, J. Zhu, R. Chong, D. Yang, W.-H. Zhang and C. Li, *J. Colloid Interface Sci.*, 2013, **393**, 58.

23 J. Burschka, N. Pellet, S.-J. Moon, R. Humphry-Baker, P. Gao, M. K. Nazeeruddin and M. Grätzel, *Nature*, 2013, **499**, 316.